CONCRETE LIBRARY OF JSCE NO. 27, JUNE 1996

ALKALI RESISTANCE OF FIBER REINFORCED PLASTIC FOR USE IN CONCRETE STRUCTURES

(Translation from Proceedings of JSCE, No.520/V-28, August 1995)

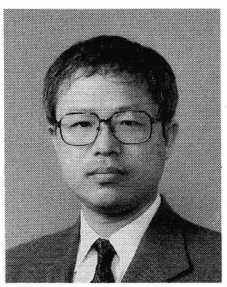
Toyo MIYAGAWA

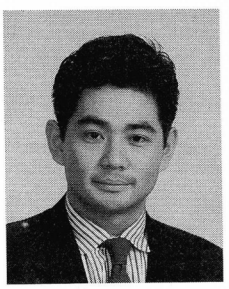
Maki YOSHIDA

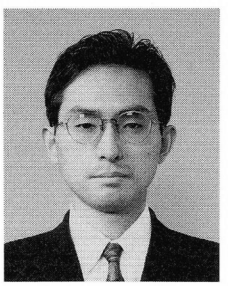
Atsushi HATTORI

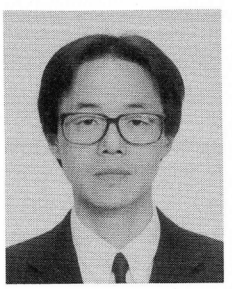
Kaoru IWAMOTO

Recently fiber reinforced plastic (FRP) has been applied as reinforcement for concrete. Few studies, however, have been conducted on its durability. This paper describes alkali resistance of some types of FRP bars. Alkali solution as an environmental media, solution temperatures and tensioning amplitude influences on mechanical properties of the FRP bars are discussed with micro structure observation and flexural testing of prestressed concrete beams.

Keywords: *fiber reinforced plastic, prestressing tendon, alkali resistance, micro crack, strength, elongation, flexural behavior of beam*

Toyo Miyagawa is an associate professor in the Department of Civil Engineering, Kyoto University, Kyoto, Japan. He received his doctorate in engineering from Kyoto University in 1985. He is the author of a number of papers dealing with durability, maintenance and repair of reinforced concrete structures. He is a member of the ACI, RILEM, CEB, JSMS, JCI and JSCE.

Maki Yoshida is a research engineer in the Construction Materials Laboratory, Institute of Construction Technological Research, Aichi Prefecture, Nagoya, Japan. He is currently engaged road maintenance within the Road Maintenance Division of Aichi Prefecture. He is a member of the JSCE.

Atsushi Hattori is a research associate in the Department of Civil Engineering, Kyoto University, Kyoto, Japan. His current research interests include application of fiber reinforcing materials to concrete structures and structural durability. He is a member of the JSMS, JCI, and JSCE.

Kaoru Iwamoto is the chief research engineer in the Development Department of Kinki Concrete Industries Co., Ltd., Osaka, Japan. His work has been associated with concrete reinforced by chopped-fibers and prestressed concrete using FRP bars as tendons. He is a member of the JSCE.

1. INTRODUCTION

Recently, many cases have been reported of the problem of premature steel reinforcement corrosion in reinforced concrete structures subjected to a chloride environment, and there has been focus on improving the situation through the use of high strength, high durability fiber reinforced plastic (FRP) as an alternative material to steel. Much research and development related to FRP application to concrete structures has been done in Japan, and in recent years some actual applications have been reported [1][2][3]. However, further research and development are needed, especially in order to obtain detailed data about the long term durability of FRP and FRP-reinforced concrete structures[4][5]. Until now reports have been made on degradation of resin due to hydrolysis in alkaline environment, chemical and/or physical degradation of interface between fiber and resin in water and/or alkaline environment[6], and degradation of fiber in an alkaline environment. However, further intensive investigations are needed to predict the long term behavior of FRP embedded in severe concrete environments subjected to high stress, such as tendons used for prestressed concrete (PC).

In this study, basic examination was conducted on the long term durability of FRP bar, which are mainly used for PC tendons, in an accelerating alkaline environment.

2. TEST PROGRAM

Experiments included immersion of FRP bars, observation of bar surface and cross section, tensile tests of bars, and flexural tests of PC beams using bars as prestressing tendons. Table 1 outlines these experiments.

2.1 Immersion

Three kinds of FRP bars presently commercially available which were expected to be durable were immersed up to 14 months in alkaline solution or tap water at specified temperatures. The FRP bars were 70 - 130cm in length, the central 30cm portions of which were immersed. They were tensioned and anchored just like prestressing tendons. The following conditions were adopted in immersion.

a) FRP bars
Mainly, one type of aramid FRP bar which has been applied to actual structures and reported to be durable against alkaline environment was examined. Two FRP bars comparable in mechanical properties were also examined. Published properties of three FRP bars are shown in Table 2.

b) Environmental Solutions
Alkaline solution (pH: 12.5 - 13.0, $Ca(OH)_2$: 2g/*l*, NaOH: 10g/*l*, KOH: 14g/*l*) was mainly used. The solution was proposed by Maruyama [7] as simulating concrete pore solution. Tap water was also used.

c) Tensioning amplitudes
Generally 0.65Pu (Pu: maximum tensile load) was adopted. 0.40Pu and 0.00Pu (not tensioned) were also given.

d) Temperatures of Environmental Solutions
20°C and 60°C were adopted. The latter with the aim of accelerating degradation.

During immersion, tensile load changes of some FRP bars were measured by center-hole load cells (capacity: 100kN) at anchorages. In addition, some acoustic emission (AE) sympathetic sensors (frequency in vibration plate-perpendicular direction: 200kHz, parallel direction: 800kHz) were attached to count ringdowns of AE. AE measurement Conditions in immersion are shown in Table 3.

2.2 Observation of Surface and Cross Section

After specified period of immersion, the FRP bars were unloaded and taken out of the solutions. Their surface and cross section were observed and their micro structure after 10 month immersion and intrusion of environmental constituents into them was investigated through Scanning Electron Microscopy (SEM) and Electron Probe Microanalysis (EPMA).

Table 1 Outline of Test Program

Solution	Alkaline Solution 60°C					Alkaline Solution 20°C					Tap Water 20°C		Not Immersed
Tension Level	0.65Pu			0.00Pu		0.65Pu			0.40Pu		0.65Pu		Not Tensioned
Immertion Period (Month)	4～5	10	14	10	14	5	10	14	10	14	10	14	
SEM/EPMA Observation		○	○		○		○		○		○	○	○
Tensile Test	○	○	○	○	○	○	○	○	○	○	○	○	○
PC Beam Flexural Test	○					○							○

○: Test conditions conducted Pu: Tensile ultimate load

Table 2 Published Properties of Fiber Reinforced Plastics

Specimen	Fiber	Matrix	Shape	Fiber Content (Vol.%)	Nominal Area (mm^2)	Guaranteed Tensile Strength (kN/mm^2)	Young's Modulus (kN/mm^2)	Elongation (%)
Aramid-T	Aramid (Technora)	Vinyl Ester Resin (Bisphenol A, Acrylic Acid, Peroxide)	Spiral Wound Round Bar (φ6)	65	28.3	1.76	53.9	3.6
Aramid-K	Aramid (Kevlar49)	Epoxy Resin (Bisphenol A, Amide)	Braided Cable (φ8)	65	50.0	1.27	63.7	2.2
Carbon	Carbon (PAN Type)	Epoxy Resin (Novolak, Amide)	Spiral Cable (φ7.5)	64	30.4	1.76	137	1.6

Table 3 AE Measurement Conditions (1)

Environmental Condition	Alkaline Sol. 60°C	Alkaline Sol. 20°C	Tap Water 20°C
Amplifer	40+30dB	40+30dB	40+20dB
Filter Through	0.2–1.0MHz	0.2–1.0MHz	0.1–1.0MHz/ 0.1–0.3MHz
Discriminate Level	250mV	150mV	250mV
Dead Time	1msec	1msec	1msec

Table 4 Grind Conditions and Ion Coating

Process	Powder	Lubricator	Time
Mechanical Grind (1)	#80(Silicon Carbide 200μm) #320(Silicon Carbide 200μm) #600(Silicon Carbide 200μm)	Water	2min. in Two Directions
Mechanical Grind (2)	#1200(Silicon Carbide 200μm) #1500(Silicon Carbide 200μm)	Water	6min. in Two Directions
Final Grind	Almina Powder (0.3μm) Almina Powder (0.06μm)	Water	10min. in Two Directions
Gold Ion Coating (5–10mA)			8min.

Table 5 SEM Conditions

Accel Voltage	2～7kV
Probe Current	6×10^{-10}A
Working Distance	10–12mm
Gun Bias	3 (Manual)

Table 6 EPMA Conditions

Area	4×4mm
Number of Pixel	200
Probe Current	$2～3 \times 10^{-8}$A
Dwell Time	60msec
Size of Pixel	20μm

Table 7 AE Measurement Conditions (2)

Amplifer	40+30dB
Filter Through	0.2～1.0MHz
Discriminate Level	150mV
Dead Time	1msec

a) Preparing Samples

The immersed FRP bars were dried at room temperature for 1 week. After being wiped with a dry cloth, the immersed central portions were cut into 2-3cm long samples for observation. A tap water lubricator, as shown in Table 4, was used in grinding and smoothing process of cross sections.

b) SEM and EPMA Observation

SEM conditions are shown in Table 5, with which mainly cross sections were examined. Intrusion of environmental constituents was investigated by EPMA for the same samples as used for SEM. EPMA conditions are shown in Table 6. Constituents to be detected were Na, K (alkaline metal), and Ca (alkaline earth metal). X-

ray amplitudes distribution given by the detected constituents were mapped with colors.

2.3 Tensile Test

a) FRP bars

Bar length was principally 50cm including, the 30cm of immersed portion and an additional 10cm at both ends in order to avoid influence of anchorages. Steel sleeves and expansive grout were used for anchoring FRP bars. For Aramid-T, the anchor sleeves used in immersion were of such a length that they were tested just as taken out, with bar length of 70cm.

b) Loading

The FRP bars were carefully set in loading direction in a loading machine by gripping both anchor sleeves. They were then subjected to simple loading at a constant rate. Loading rate was A × Vf × (500 ± 50) N (A: nominal area, Vf: volume fraction of fibers in tensile direction) per minute to maintain uniform for all fiber types. Some Aramid-T were cyclicly loaded, with unloading at each 9.8kN enlargement in order to obtain Felicity ratio of Kaiser effect.

c) Measurement

Load, strain, and AE ringdowns were respectively measured by a load cell, attached strain gauges, and AE sensors. An AE sensor as used in immersion was attached at the middle of the immersed portions of each FRP bar. Conditions of tensile test AE measurements in tensile test are shown in Table 7. Fracture surface observation was also conducted.

2.4 PC Beam Flexural Test

Post-tensioned PC beams were provided using immersed and not immersed FRP bars as tendons. The influence on load carrying behavior of FRP bar degradation due to immersion are investigated.

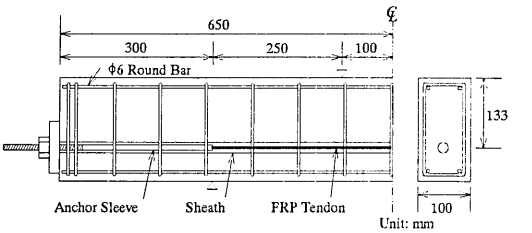

Fig. 1 Prestressed Concrete Beam Specimen

Table 8 Mix Proportion of Concrete

Design Strength	NMS	Sl.	Air	W/C	s/a	Unit mass (kg/m³)				WRA
(MPa)	(mm)	(cm)	(%)	(%)	(%)	W	C	S	G	(cc/m³)
40	15	5±1	3	56	42	175	315	740	1087	788

Table 9 Test Conditions of PC Beams

Specimen	Tendon		Prestress Level
T-N-1	Aramid-T	Not Immersed/Not Tensioned	0.65Pu (32.5kN)
T-N-2			
T-2-1		Alkaline Sol.20°C 0.65Pu 4mon.	
T-6-1		Alkaline Sol.60°C 0.65Pu 4mon.	
T-6-2			
K-N-1	Aramid-K	Not Immersed/Not Tensioned	0.65Pu (41.2kN)
K-N-2			
K-6-1		Alkaline Sol.60°C 0.65Pu 4mon.	

Table 10 Mechanical Properties of Concrete

Compressive Strength (MPa)	Young's Modulus (×10⁴MPa)	Flexural Strength (MPa)	Tensile Strength (MPa)
45.2	3.51	5.77	2.65

Table 11 Mix Proportion of Grout

W (kg)	C (kg)	WRA (g)
3.5	10	150

a) PC Beams

A total of 8 PC beams (width × height × total length = 10 × 20 × 130cm) were provided. The beams were designed to show flexural tensile fracture (fracture by failure of a tendon) when the each FRP bars without immersion / tensioning were used as tendons. Static load was applied by unidirectional two point symmetric loading. Dimensions of PC beams and the mix proportion of concrete, which had a design compressive strength of 40MPa, are shown in Fig. 1 and Table 8. FRP bars used as tendons were Aramid-T and Aramid-K either without immersion / tensioning or immersed in 20°C or 60°C alkaline solutions for 4-5 months with 0.65Pu. Prestressing load was 0.65Pu of each original bar. Flexural span was the central 20cm to show the influence of immersed portion (30cm), and loading span was 70cm to avoid anchrage influences. Details of the PC beams and results of concrete strength when loading are shown in Tables 9 and 10.

Prestress was introduced at 2 weeks after checking concrete compressive strength. All PC beams were immediately grouted, and then cured in a room for another 2 weeks. Grout mix proportion is shown in Table 11.

b) Measurement

The following items were measured during loading.

(1) Load: measured by a load cell (capacity: 300kN).

(2) Deflection: measured by one displacement transducer at mid span (capacity: 10mm) and two for both supports (capacity: 5mm). Mid span deflection was obtained by subtracting average of supports displacements from that of mid span.

(3) Crack Width: measured by 5 π-shaped crack gauges (length: 50mm, capacity: 2mm) placed in flexural span at tendon depth (d = 133mm).

3. DURING IMMERSION

3.1 Relaxation

Relaxation of FRP bars immersed with tensioning are shown in Fig. 2. No FRP bar was fractured during immersion.

All FRP bars relaxed in proportion to logarithm of time. However, relaxation in 60°C alkaline solution was accelerated from beginning of immersion (indicated by dots in Fig. 2). Tensile forces decreased for a while, but subsequently increased slightly after some 4000 hours rather than decreasing further. Reductions in tensile forces of Aramid-T by 9000 hours were approximately 13% when immersed in 60°C alkaline solution, 11% in 20°C alkaline solution, and 8.5% in 20°C tap water.

Linear regression gradients of relaxation from beginning of immersion to 3000 hours are shown in Table 12. Relaxation progressed most rapidly in 60°C alkaline solution with 0.65Pu, of which the relaxation rate was never less than twice those in 20°C alkaline solution with the same tensioning. Aramid-T and Aramid-K had larger relaxation rate in 20°C alkaline solution than 20°C tap water, and subjected to 0.65Pu than 0.40Pu.

Relaxation may be taken as an index to characterize the influences of immersion and tensioning on mechanical properties of FRP bars. Relaxation increases most in 60°C alkaline solution on the same tensioning condition, and 20°C alkaline solution, 20°C tap water have less influence in this order, and small tensile loads have little affect.

3.2 Total Count of AE Ringdowns

Total count of AE ringdowns during immersion are shown in Fig. 3. AE ringdowns appeared from initial

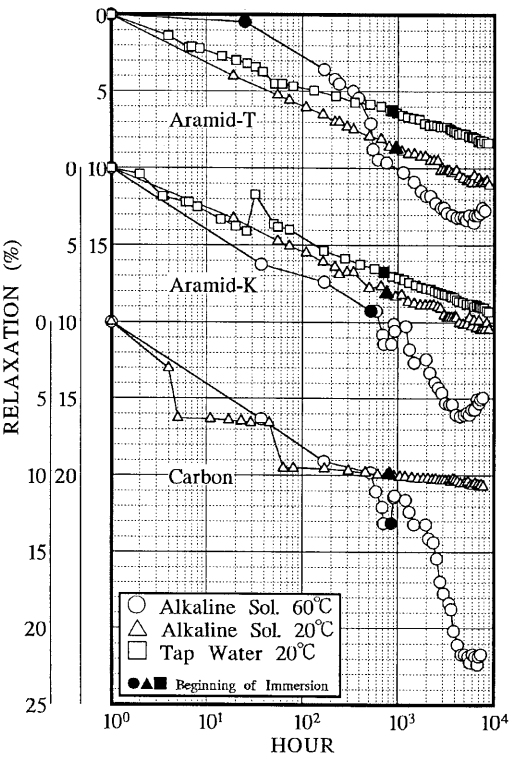

Fig. 2 Relaxation under Immersion (0.65Pu)

Table 12 Relaxation Rate under Immersion

Environmental Conditions		Atamid-T	Aramid-K	Carbon
Alkaline Sol. 60°C	0.65Pu	5.45	11.0	12.8
Alkaline Sol. 20°C	0.65Pu	2.48	2.26	0.68
	0.40Pu	1.33	2.03	-
Tap Water 20°C	0.65Pu	2.03	2.22	-

Unit: %/Log(hour)

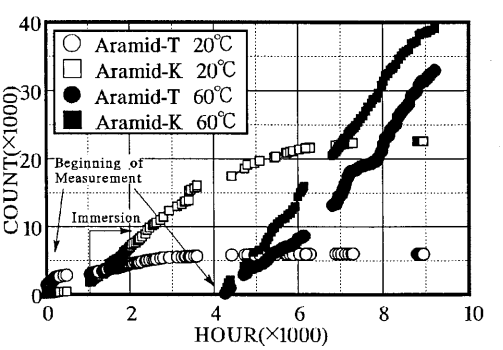

Fig. 3 AE Count under Alkaline Immersion (0.65Pu)

tensioning, although total count varied, and then count rate decreased after some time. By beginning immersion, count rates was accelerated, where the rate of Aramid-K was larger than Aramid-T. Subsequently, while count rates decreased again in 20°C alkaline solution as the time proceeded, no significant reductions of count rates were observed in 60°C alkaline solution from some 4000 hours after initial tensioning to 9000 hours when immersion ended. In this period, almost constant count rates were measured in both FRP bars.

Increase of count rates by immersion indicates that intrusion of environmental solution invoked internal microfractures which causes AE ringdowns. The microfracturing was accelerated more in 60°C alkaline solution than in 20°C, as Fig. 3 shows. This means acceleration by high temperature.

4. OBSERVATION OF SURFACE AND CROSS SECTION

By examining resin surface, existence of internal cracks and cross sectional distributions of constituents in alkaline solutions, two types of degradation processes were observed in the FRP bars used in this study; they were, (1) generation of deteriorated layer near surface due to sorption of environmental constituents, and (2) surface softening due to dissolution of resin causing loss of surface layer accompanying reduction of stress transfer among longitudinal fibers.

4.1 Generation of Deteriorated Layer

As shown in Fig. 4, cracks were observed in immersed Aramid-T cross sections in fiber-resin interfaces. These cracks connected along the surface into a large crack as shown in Fig. 5. Distribution of environmental constituents obtained by using EPMA showed that both K and Na intruded inside and K tended to progress farther, while Ca stayed near surface. Taking this into consideration, K can be singled out as a typical intruding constituent. Distribution of K in cross section of Aramid-T immersed in 60°C alkaline solution with 0.65Pu after 9000 hours is shown in Fig. 6. K is found inside to some extent, especially concentrated around a large crack of about 500μm width. Since tap water was used as lubricator in grinding and smoothing cross section before EPMA observation in this study, environmental constituents detected by EPMA are jointed firmly as chemical bonds. In other words, they did not exist merely via cracks, but had close relations with resin property changes. Larger tensile loads also tended to cause inward cracks and environmental constituents correspondingly

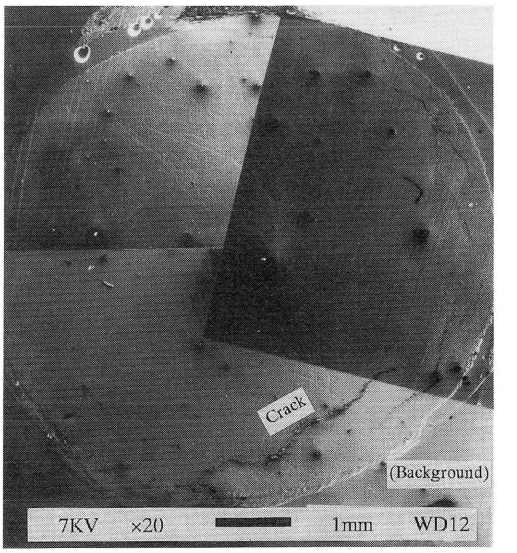

Fig. 4 Example of Section of Aramid-T (Alkaline Sol. 60°C 0.65Pu)

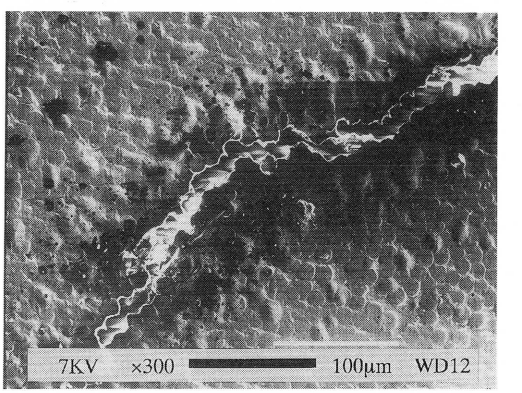

Fig. 5 Crack in Aramid-T (Alkaline Sol. 60°C 0.65Pu)

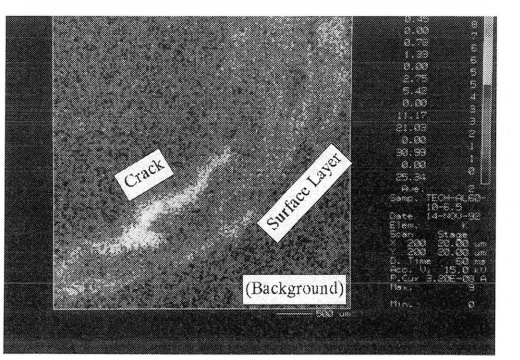

Fig. 6 Distribution of Potassium (K) in Aramid-T (Alkaline Sol. 60°C 0.65Pu)

distributed farther inside.

4.2 Surface Softening

Aramid-K and Carbon cross sections are shown in Fig. 7 and 8. Distribution of K in the same cross section of Aramid-K is shown Fig. 9. Little K was detected in Carbon. These figures indicate that both FRP bars are not aggressive, regardless of tensioning amplitude, but proceed degradation by surface softening. Surface softening in Aramid-K subjected to large tensioning amplitude was reduced to some degree. Since Aramid-K has braided structure, this was possibly caused by compression in distance among fibers. On the other hand, notable surface softening was observed in Carbon, as shown in Fig. 10. Deformed surface layer of spiral fiber winding was peeled off after 9000 hours immersion, partly as deep as longitudinal fibers. The layer of spiral fiber winding was so softened as to lose connection to body and mostly peeled off by wiping with a dry cloth.

4.3 Degradation Processes of Aramid-FRP bars

Aramid-T is reported to have superior fiber durability in alkalinity, so that intrusion of environmental constituents near fibers might not cause critical strength degradation. However, influence of internal cracks, such as shown in Fig. 5, and/or sorption of constituents in actual situations are yet to be investigated.

As aramid-K is reported to have some degree of fiber durability problems in high alkalinity[8], fiber should be separated from alkalinity. Although results indicate that intrusion depth of environmental constituents is limited to near the surface, progress of degradation and local intrusion through pin-holes in resin could cause strength reduction over a longer period.

5. TENSILE TEST

5.1 Aramid-T

a) Tensile Strength and Young's Modulus

Results of tensile tests are shown in Table 13. No dramatic reduction of tensile strength was seen, and all Aramid-T specimens satisfied the guaranteed strength. However, although quantitative evaluation is difficult because of insufficient number of specimens, some specimens did lose tensile strength.

Young's modulus, which was obtained by linear regression of each stress-strain curve in apparently linear regions with stress corresponding to less than 0.65Pu, varied to some extent. That is, it increased in

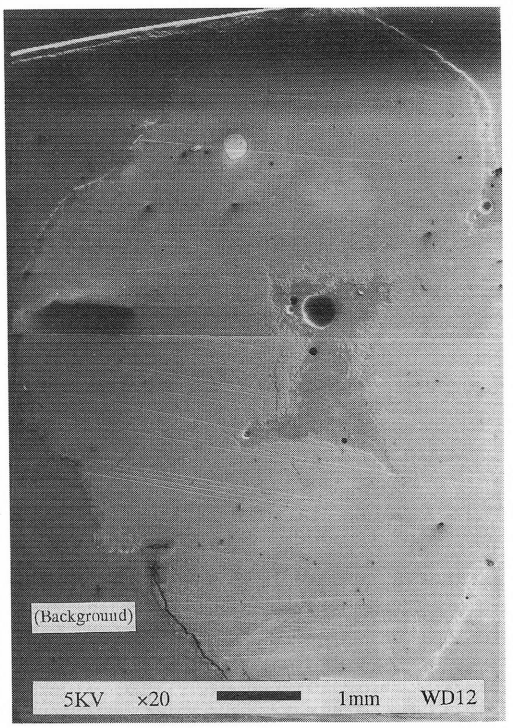

Fig. 7 Example of Section of Aramid-K (Alkaline Sol. 60°C 0.65Pu)

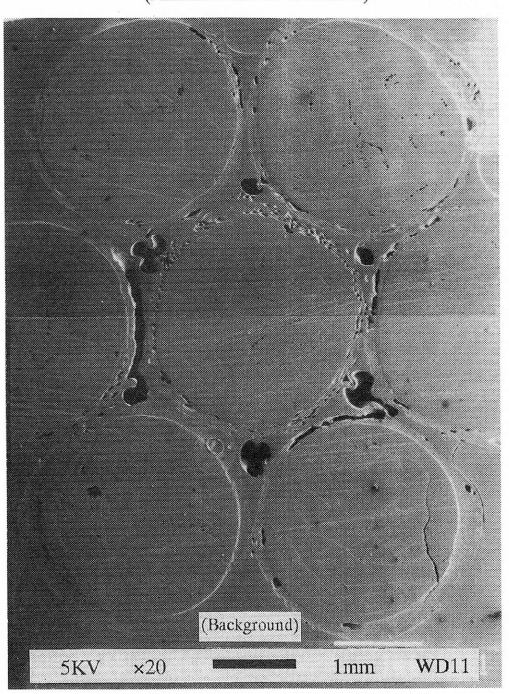

Fig. 8 Example of Section of Carbon (Alkaline Sol. 60°C 0.65Pu)

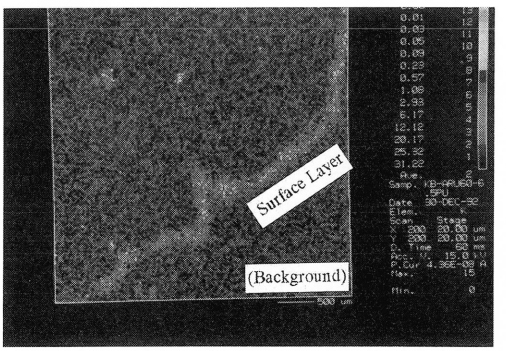

Fig. 9 Distribution of Potassium (K) in Aramid-K (Alkaline Sol. 60°C 0.65Pu)

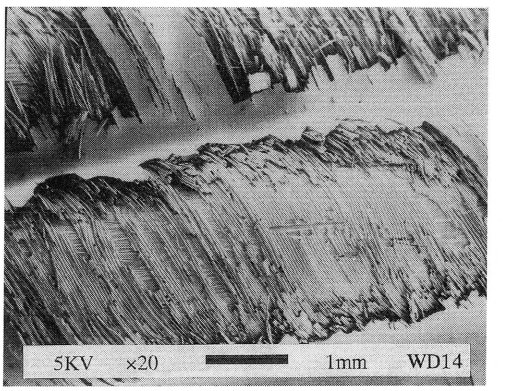

Fig. 10 Example of Surface of Carbon (Alkaline Sol. 60°C 0.65Pu)

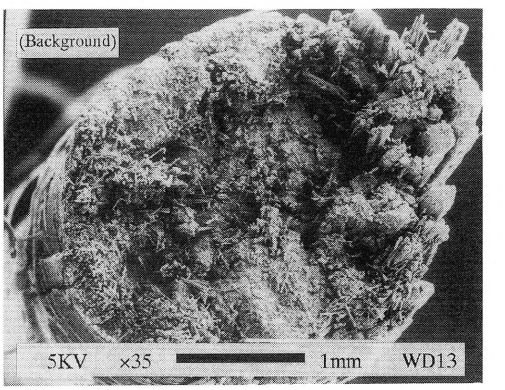

Fig. 11 Fracture Surface of Carbon (Not Immersed/Not Tensioned)

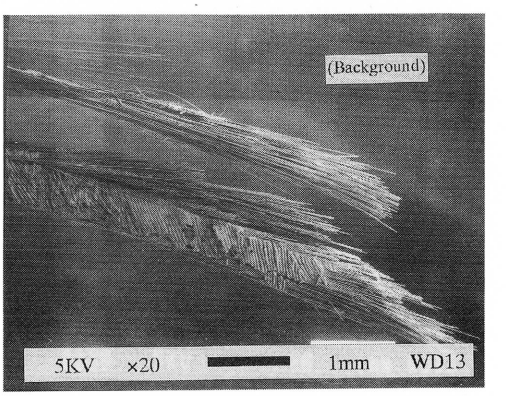

Fig. 12 Fracture Surface of Carbon (Alkaline Sol. 60°C 0.00Pu)

immersed Aramid-T with tensioning, and, on the contrary, decreased in those immersed without tensioning, as compared with those without immersion / tensioning. As Table 13 shows, while the largest Young's modulus increase is in the FRP bar immersed in 60°C alkaline solution with 0.65Pu after 10 months (+11%), the largest decrease (-17%) is found after 14 months in that of 60°C without tensioning. Therefore, although Young's modulus of Aramid-T decreases by immersion, it tends to increase to some extent by tensioning.

b) Count Rate of AE Ringdowns

Count rates of AE ringdowns during tensile testing are shown in Fig.13. Existence of Kaiser effect was examined on Aramid-T without immersion / tensioning and on that immersed in 60°C alkaline solution with 0.65Pu for 9000 hours by applying cyclic tensile load. As Fig. 14 shows, the former showed clear Kaiser effect in a small load stage and Felicity ratio indicating internal stability was exceeded 0.95[9]. Kaiser effect afterwards became ambiguous with increase of applied load so that Felicity ratio fell behind 0.95 beyond 0.70Pu. On the other hand, the latter did not show clear Kaiser effect after the small load stage. Accordingly, the Felicity ratio was relatively small and reduced with increase of applied load. This indicates existence of unstable portions inside immersed Aramid-T.

Relative energies (1V × 1V × 1ms = 1 count) obtained by AE amplitude and duration time are shown in Fig. 15. Almost constant energy distribution was observed in Aramid-T without immersion / tensioning from 0.30Pu through fracture. Relatively large energies arised since their initiation. On the other hand, in those immersed in 60°C alkaline solution with 0.65Pu, although AE initiated immediately after loading began, most relative energies were small. Therefore, unstable portions inside Aramid-T resulting in unclear Kaiser effect are not in principal load carrying sections controlling tensile strength,

Table 13 Results of Tensile Test

Environmental Condition			Aramid-T		Aramid-K		Carbon	
Solution	Tension Level	Immersion Period (Month)	Tensile Strength (kN/mm^2)	Young's Modulus (kN/mm^2)	Tensile Strength (kN/mm^2)	Young's Modulus (kN/mm^2)	Tensile Strength (kN/mm^2)	Young's Modulus (kN/mm^2)
Not Immersed/Not Tensioned			1.96 (1.00)	55.1 (1.00)	1.41 (1.00)	64.3 (1.00)	1.97 (1.00)	154.5 (1.00)
Tap Water 20°C	0.65Pu	10	1.91 (0.97)	54.1 (0.98)	-	-	-	-
		14	1.96 (1.00)	56.7 (1.03)	1.43 (1.01)	62.7 (0.98)	2.10 (1.07)	136.7 (0.88)
Alkaline Sol. 20°C	0.40Pu	10	1.79 (0.91)	46.5 (0.84)	-	-	-	-
		14	-	-	1.44 (1.02)	63.0 (0.98)	-	-
	0.65Pu	5	1.92 (0.98)	57.0 (1.03)	-	-	-	-
		10	1.94 (0.99)	58.5 (1.06)	-	-	-	-
		14	1.89 (0.96)	40.2 (0.73)	1.53 (1.09)	64.7 (1.01)	2.00 (1.15)	151.2 (0.98)
Alkaline Sol. 60°C	0.00Pu	10	1.88 (0.96)	47.1 (0.85)	-	-	1.86 (0.94)	114.4 (0.74)
		14	1.93 (0.98)	45.6 (0.83)	1.26 (0.89)	72.2 (1.12)	1.81 (0.92)	126.1 (0.82)
	0.65Pu	4~5	1.80 (0.92)	53.3 (0.97)	1.44 (1.02)	62.7 (0.98)	1.94 (0.98)	128.0 (0.83)
		10	1.85 (0.94)	61.3 (1.11)	-	-	-	-
		14	-	-	1.37 (0.97)	68.5 (1.07)	1.92 (0.97)	127.3 (0.82)

( ): Ratio to the specimen without immersion/tensioning

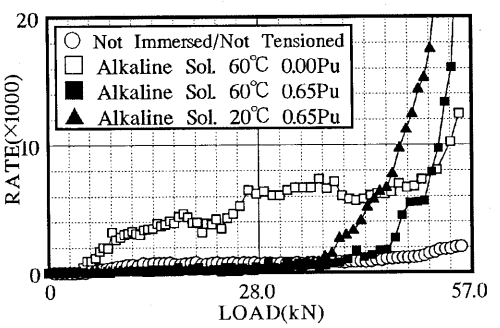

Fig. 13 Example of Count Rate of AE (Aramid-T)

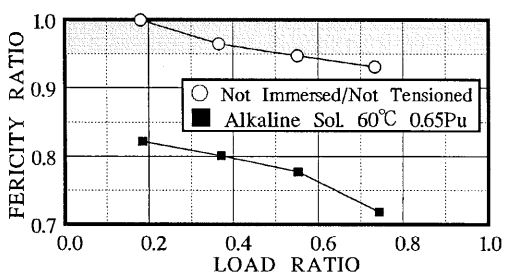

Fig. 14 Fericity Ratio (Aramid-T)

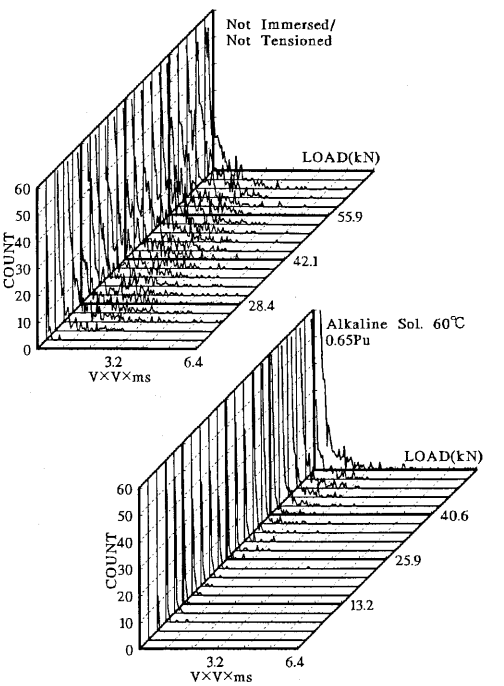

Fig. 15 Relative Energy Count (Aramid-T)

but rather in processed surfaces (spiral winding), deteriorated resin and/or damaged interfaces. Most energies were also small beyond the previously applied tensile load during immersion, and large energies were observed only near fracture.

To summarize these results, while Aramid-T is stabilized in tension by immersion and tensioning in a short period, as indicated by increased Young's modulus, unstable portions are invoked in cross section after longer immersion. However, the unstable potions are not so critical as to reduce Aramid-T tensile strength.

Table 14 Results of Beam Test

Specimen	Cracking Load (kN)	Maximum Load (kN)	Displacement at Maximun Load (mm)	Failure Mode
T-N-1 T-N-2	41.7 (1.00)	110.7 (1.00) [91.8]	7.54 (1.00)	I
T-2-1	42.1 (1.01)	105.4 (0.95) [91.1]	6.10 (0.81)	I
T-6-1	44.4 (1.06)	96.7 (0.87) [89.0]	3.19 (0.42)	II
T-6-2	46.3 (1.11)	102.6 (0.93) [89.0]	4.20 (0.56)	II
K-N-1 K-N-2	55.0 (1.00)	126.2 (1.00) [106.2]	5.33 (1.00)	I
K-6-1	56.7 (1.03)	130.2 (1.03) [106.9]	5.63 (1.05)	I

( ): Ratio to the specimen without immersion/tensioning

[ ]: Calculated value

Failure Mode: I: Flexural Tensile, II: Flexural Compressive

5.2 Aramid-K and Carbon

Although Aramid-K showed surface softening degradation, the degree of degradation was not so great that changes in tensile properties after immersion were not significant. The changes in tensile properties showed good correlation with surface softening state; that is, larger tensile load caused smaller degree of surface softening.

Some Carbon with observed surface softening showed reduction in tensile strength and/or Young's modulus. All Carbon, however, satisfied the guaranteed strength. For fracture mode, damages were concentrated in a certain cross section, as shown in Fig.11, in Carbon without immersion / tensioning, and few fiber pull-outs were observed in fracture surfaces, due to firm fiber-resin interface. On the other hand, after immersion as shown in Fig. 12, fracture surface with many fiber pull-outs was observed, so that a wide region was damaged. This was mainly caused by deterioration of spiral fibers wound around longitudinal surface fibers, reducing longitudinal fiber binding force.

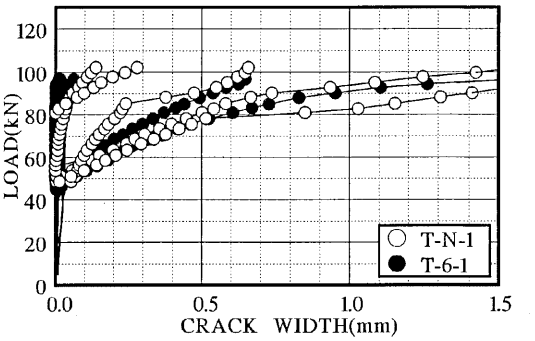

Fig. 16 Crack Width (Aramid-T)

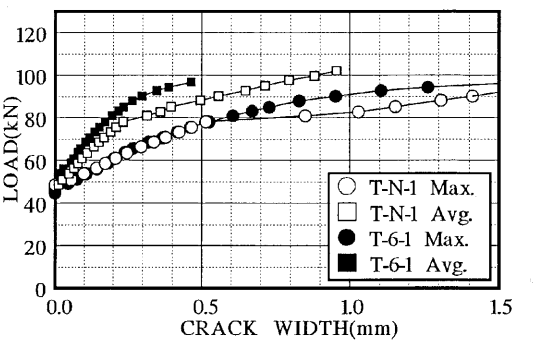

Fig. 17 Maximum and Averaged Crack Width (Aramid-T)

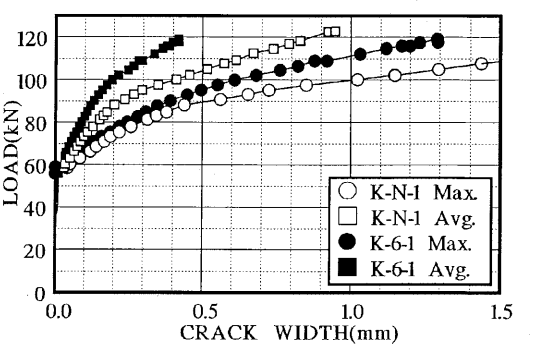

Fig. 18 Maximum and Averaged Crack Width (Aramid-K)

6. PC BEAM FLEXURAL TEST

6.1 Crack Behavior

As shown in Table 14, flexural cracking loads of PC beams using immersed Aramid-T and Aramid-K slightly increased, partly due to increased Young's modulus of tendons.

Crack width of PC beams using Aramid-T is shown in Fig. 16. Poor crack distribution was observed with immersed tendon in 60°C alkaline solution for 4 months, as compared with that without immersion / tensioning. This can also be recognized by Fig. 17 showing average and maximum crack width. Differences between average

and maximum crack width at a certain average crack width is larger with immersed specimens because few cracks resulted in widened maximum crack width. Degraded tendon bond strength might have reduced crack distribution.

Reduction of crack distribution was also observed in the PC beam using immersed Aramid-K as shown in Fig. 18. Bond degradation might also have affected the behavior here.

6.2 Maximum Load and Failure Mode

The largest decline of Maximum load was 10kN (approximately 10%) in an immersed Aramid-T PC beam. Deflection at maximum load also decreased.

As shown in Table 14, first, PC beams with Aramid-T immersed in 60°C alkaline solution lost loading capacity accompanied with slight compressive failure of concrete in the compression zone (flexural compressive failure). They then completely fractured by tensile failure of the tendons. The other PC beams failed by initial tendon tensile failure (flexural tensile failure), as design. Failure mode shift to flexural compressive failure in the former beams was caused by an increase of extreme fiber stress in compression zone concrete corresponding to increasing stress carried by the tendons in the same strain, since the immersed tendons might have an increased Young's modulus.

In this way, changes in FRP bar properties due to degradation, which could be negligible in a simple tensile test, can affect behavior of actual members, although it is difficult to discuss the influence of tendon tensile properties on maximum load and deflection because they are affected by fracture modes. For example, when a large interfacial stress is transfered by matrix resin between a tendon and concrete in a concrete structure, and/or when a longitudinal tendon is bent in some curvature along with beam deflection, certain PC beam behavior is liable to be affected by property changes of the tendon.

7. CONCLUSION

Judging from the results obtained from tensile test after 9000 hours immersion with tensioning, no dramatic degradation of tensile properties such as tensile strength was detected in any type of FRP bar examined in this study. Together with consideration that accelerating environmental conditions adopted in this study were more severe than conditions in general concrete, their durability might be promising. However, some changes of internal microstructure were also recognized, which will possibly cause some type of property deterioration, though they have less significance at present.

Internal structure changes mainly consisted of interfacial cracks between fiber and binding resin. This indicates that separate investigations of fiber and resin degradation processes are not necessarily sufficient to clarify the durability of composite FRP bars.

The main results obtained in this study are summarized as follows:

(1) Alkaline solution have greater influences on FRP bar degradation than tap water. K and Na, alkaline metals, show similar behavior in intruding FRP bars, and K tend to be more aggressive. On the other hand, Ca, alkaline earth metal, is less aggressive than other two constituents, existing only along surfaces and widely cracked areas.

(2) 60°C alkaline solution caused the same degradation process as 20°C and is therefore useful for accelerating.

(3) Sorption of alkaline solution were observed in Aramid-T, a bundle of parallel fibers, and internal cracks were detected correspondingly, accelerated by tensile stress. However, Aramid-T shows durable tensile behaviors because of high durability and good longitudinal fiber orientation. uence of interaction between Aramid-T and concrete on behavior of a reinforced concrete members should be investigated further.

(4) Alkaline solution intrudes little into Aramid-K, with some advantage due to its braided shape. However, fiber durability against high alkalinity must still be improved. Degradation of Carbon is also found within surface layers. However, deterioration of resin and/or spiral fiber on surfaces can cause reduction of mechanical properties.

(5) FRP bar degradation possibly influences load carrying behavior of a concrete member, although tensile strength of the FRP bar decreased little.

Further, long term investigation should be done on the relationship of accelerating environment of room and high temperature alkaline solutions used in this study with actual environment in concrete, and on the influence on bond behavior of degradation of an FRP bar embedded in concrete on bond behavior.

Acknowledgment

The authors wish to express their cordial gratitude to Prof. Manabu Fujii and Dr. Susumu Inoue (Kyoto University) for their earnest supervison and collaboration, and Mr. Tatsuo Kawahigashi (Kinki University) for his cooperation in using EPMA. The FRP bars were provided by members of the Association of Composites Materials Using Continuous Fiber for Concrete Reinforcement (CCC). Their strong support has been sincerely appreciated.

References

[1] Kobayashi, K., "Application of Advanced Composite Materials to Concrete Construction", Proc. of JSCE, No.420/V-13, pp.17-28, 1990.8. (in Japanese)

[2] Hiraga, Y., "Why FRP ? 3. Grid-shaped Composite Materials for Concrete Structures", Reinforced Plastics, Vol.34, No.6, pp.207-215, 1988.6. (in Japanese)

[3] Rokugou, K. and Mashima, M., "Polymers in Concrete -Recent Development- 5. Recent Development of Fiber Reinforcing Materials for Concrete Structures", Journal of the Society of Materials Science, Japan, Vol.41, No.471, pp.1817-1822, 1992.12. (in Japanese)

[4] JSCE, "Application of Continuous Fiber Reinforcing Materials to Concrete Structures", Concrete Library No.72, 1992.4. (in Japanese, translation available in Concrete Library International of JSCE No.19, 1992.7 and Concrete Engineering Series of JSCE No.3, 1993.10)

[5] Advanced Composite Materials Research Committee of AIJ, "State-of-the-Art Report on Advanced Composite Materials for Concrete Structures", 1989.3. (in Japanese)

[6] Weitsman, Y., "Moisture Effects and Moisture-induced Damage in Polymeric Composite", Composite Materials and Structures, pp.111-120, 1988.

[7] Maruyama, T., "Experimental Reserach into the Use of Carbon Fiber Reinforced Plastic Rods for Concrete Reinforcement", Dr. Eng. Theses, Univ. of Tokyo, 1991.3. (in Japanese)

[8] Iwamoto, K., Agawa, T., Uchida, Y. and Yoshikawa, F., "Basic Properties of FRP Bars for Concrete Reinforcement", JSCE Kansai Chapter, Proc. of Annual Conference of Civil Engineers, V-28, 1989.5. (in Japanese)

[9] Corton, H.T., "Micromechanics and Fracture Behavior of Composites", Modern Composites Mateirals, pp.27-105, 1967.

[10] Okuda, S., "Latest Reformation and Stabilize Rechnique for Avoiding Degradation and Collapse of Polymers", Polymers Research Society, 1981.5. (in Japanese)

[11] Hojo, H., Tsuda, K. and Ogasawara, T., "Degradation Processes of Durable Resins Used for FRP", Reinforced Plastics, Vol.34, No.2, pp.49-54, 1988.2. (in Japanese)

[12] Hull, D., "An Introduction to Composite Materials", Syndicate of the Cambridge University Press, England, 1982 (Japanese version by Miyairi, H., Ikegami, K., and Kinbara, I., Baifukan, 1984

[13] Polymers-in-Concrete Committee, "State-of-the-Art Report on Painting Floors in Food Factories", Japan Sciety of Industrial Techniques Promoters, 1992.9. (in Japanese)

[14] Uomoto, T., and Nishimura T., "Properties of Fiber Plastic Rods for Prestressing Tendons of Concrete (1) - Tensile Strength and Variation-", Monthly Jour. of Institute of Industrial Science, University of Tokyo, Vol.42, No.5, pp.290-293, 1990.5. (in Japanese)